

# Structural, optical and electrical properties of $\text{Sb}_2\text{O}_3$ thin films with different thickness

N. TIGAU\*, V. CIUPINA<sup>a</sup>, G. PRODAN<sup>a</sup>

*Faculty of Science, "Dunarea de Jos" University, Galati, R-800201, Romania*

*<sup>a</sup>"Ovidius" University, Constanta, R-900527, Romania*

Thin films of  $\text{Sb}_2\text{O}_3$  with different thickness ( $d=0.20\text{-}1.10\ \mu\text{m}$ ) were deposited onto glass substrates by thermal evaporation technique. The structural, optical and electrical properties were investigated and the effect of films thickness on films properties was discussed. The transmission electron microscopy (TEM) analysis revealed that the  $\text{Sb}_2\text{O}_3$  thin films are polycrystalline and have a cubic structure. The small values of the roughness obtained from atomic force microscopy (AFM) measurements, ranging from 4.7 to 17.6 nm, show relatively smooth surfaces. The spectral absorption coefficient and optical band gap energy of the  $\text{Sb}_2\text{O}_3$  thin films at the fundamental absorption region were determined using the spectral data of transmittance measurements in the wavelength range 250-1400 nm. Temperature dependence of the electrical conductivity was studied in a wide range, 289-445 K. It is observed that the electrical conductivity of  $\text{Sb}_2\text{O}_3$  thin films tend to increase with increasing of the film thickness. Also, it is observed that the surface defects in thinner films could play a more important role in the effect on optical and electrical properties. For thicker films the grain boundary could play a more important role in the effect on films properties.

(Received October 14, 2005; accepted January 26, 2006)

*Keywords:* Antimony trioxide, Thin films, Optical band gap, Electrical conductivity

## 1. Introduction

Thin antimony trioxide ( $\text{Sb}_2\text{O}_3$ ) films are of importance due to their unique optical and physical properties. They have a wide variety of applications, such as a high-efficiency flame-retardant synergist in plastics, paints and adhesives [1,2]. Also, they are used as wonderful ultraviolet filters for interferometric applications [3,4].  $\text{Sb}_2\text{O}_3$  glasses have been studied as they present extended infrared transmission [5]. Several studies have been focused on optical properties mainly non-linear optical properties as they present higher refractive index [3,5]. The main property of  $\text{Sb}_2\text{O}_3$  for these applications is due to the polymorph nature of the crystalline structure of  $\text{Sb}_2\text{O}_3$  thin films. At room temperature the stable solid phase of  $\text{Sb}_2\text{O}_3$  is the cubic senarmonite, which contains the  $\text{Sb}_4\text{O}_6$  molecule, whereas the high temperature orthorhombic phase valentinite has a polymeric sheet structure built up from eight-member  $\text{Sb}_4\text{O}_4$  rings [6]. Therefore, it is necessary to establish the relationship between the preparation conditions and the optical and electrical properties of  $\text{Sb}_2\text{O}_3$  thin films for electronic or optoelectronic applications. Electronic transport and optical properties of  $\text{Sb}_2\text{O}_3$  thin films strongly depend on the deposition parameters.

In our recent papers [7-10], we have studied the influence of substrate temperature and post-deposition heat treatment on the structural, optical and electrical characteristics of  $\text{Sb}_2\text{O}_3$  thin films. In this paper we extended these investigations by approaching the thickness dependence of structural, optical and electrical properties

on the  $\text{Sb}_2\text{O}_3$  thin films deposited onto glass substrates, maintained at room temperature, by thermal vacuum evaporation technique.

## 2. Experimental

Polycrystalline  $\text{Sb}_2\text{O}_3$  thin films were deposited onto well-cleaned glass slides substrates kept at temperature  $T_s = 289\ \text{K}$ , by thermal evaporation under vacuum. The studied samples were obtained by evaporation of high-purity  $\text{Sb}_2\text{O}_3$  powder (99.99 % from Merck) in a standard vacuum unit maintaining  $2 \times 10^{-5}$  Torr residual pressure. Quartz crucible with the charge was used as an evaporation source. The temperature of the evaporation source was  $656\ ^\circ\text{C}$  and the deposition rate was about  $10\ \text{\AA}/\text{s}$ . The glass substrates were placed at 10 cm above the source, with the surface being perpendicular to the vapor flux. By modification of the deposition time films in the same experimental conditions but having different thickness was prepared. The thickness of the deposited films was determined by an interferometric method [11], to an accuracy of  $\pm 10\ \text{nm}$  and the investigated samples ranged between  $0.20\ \mu\text{m}$  and  $1.10\ \mu\text{m}$ .

The microstructure of the  $\text{Sb}_2\text{O}_3$  thin films was investigated by transmission electron microscopy (TEM). TEM measurements were made using a higher resolution electron microscope, Philips CM 120, operating at an accelerating voltage of 100 kV and capable of a point-to-point resolution of  $2\ \text{\AA}$ . Electron diffraction patterns were also recorded, in order to investigate the structural

change of  $\text{Sb}_2\text{O}_3$  thin films as a function of film thickness. The surface morphology of thin films was studied by atomic force microscopy (AFM).

Optical transmission studies were carried out to estimate the band gap of the  $\text{Sb}_2\text{O}_3$  thin films using a UV-VIS—NIR double-beam spectrophotometer (model PMQ II, Carl Zeiss Jena) in the wavelength range between 250-1400 nm. For this purpose, the sample deposited on the glass substrate was placed in front of the sample beam and the identical glass slide was placed in front of the reference beam.

For the electrical measurements,  $\text{Sb}_2\text{O}_3$  thin films were deposited onto glass substrates previously equipped with coplanar aluminium electrodes that form ohmic contact with  $\text{Sb}_2\text{O}_3$  and deposited by thermal evaporation under vacuum of  $2 \times 10^{-5}$  Torr. A 6517 A Keithley electrometer was used for resistance measurement in the temperature range of 289 - 445 K. The electrical conductivity was determined according to the relation  $\sigma = \ell / (Rbd)$ , where  $\ell = 3$  mm is the distance between the aluminium electrodes,  $R$  represents the measured electrical resistance of the film,  $b = 1.5$  was the width of the  $\text{Sb}_2\text{O}_3$  thin films and  $d$  is the thickness of the films [12,13].

### 3. Results and discussion

#### 3.1. Structural characteristics of the films

The  $\text{Sb}_2\text{O}_3$  thin films prepared under optimum conditions on glass substrates were physically stable and had very good adhesion to the substrate. In order to examine the structure of the films, selected area electron diffraction (SAED) patterns and diffraction contrast images were taken. Typical SAED from representative  $\text{Sb}_2\text{O}_3$  thin films with a thickness of  $0.20 \mu\text{m}$  is shown in Fig. 1 [14]. The SAED patterns obtained from all studied samples with film thickness range between  $0.20 \mu\text{m}$  and  $1.10 \mu\text{m}$  were the same.

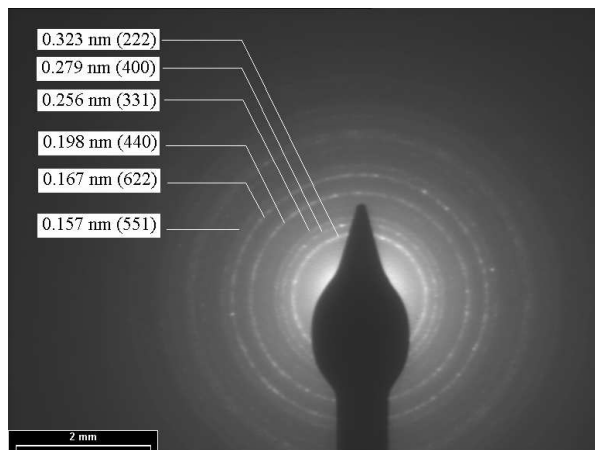


Fig. 1. Typical SAED pattern of  $\text{Sb}_2\text{O}_3$  thin films ( $d = 0.20 \mu\text{m}$ ).

The sharper rings in the SAED pattern (Fig. 1) indicate the polycrystalline nature of the  $\text{Sb}_2\text{O}_3$  thin films. The diffraction rings shown in this pattern are corresponding to an lattice spacing of 0.323 nm, 0.279 nm, 0.256 nm, 0.198 nm, 0.167 nm and 0.157 nm which fits well with those of the (222), (400), (331), (440), (622) and (551) planes, respectively, of the cubic phase of  $\text{Sb}_2\text{O}_3$ . The calculated lattice parameter was found to be 11.145 Å, in good agreement with the value of 11.152 nm reported from the standard XRD data file (JCPDS 5-0534) for  $\text{Sb}_2\text{O}_3$  cubic phase.

Fig. 2a and b are bright-field transmission electron microscopy (BF-TEM) images recorded from plan view specimens, showing that both the thinner film ( $d = 0.20 \mu\text{m}$ ) and thicker film ( $d = 1.10 \mu\text{m}$ ) exhibits a grainy structure which consists of many small grains of relatively uniform size forming a morphologically homogeneous films. The size distributions of the crystallites, obtained from measurements on around 400 grains, are plotted in Fig. 3. The distributions of grain sizes, as measured from BF-TEM images, were fitted to the lognormal curves [8,15,16]. The mean grain size,  $D_m$ , in the thinner film (7.59 nm) is significantly smaller than that in thicker films (39.10 nm).

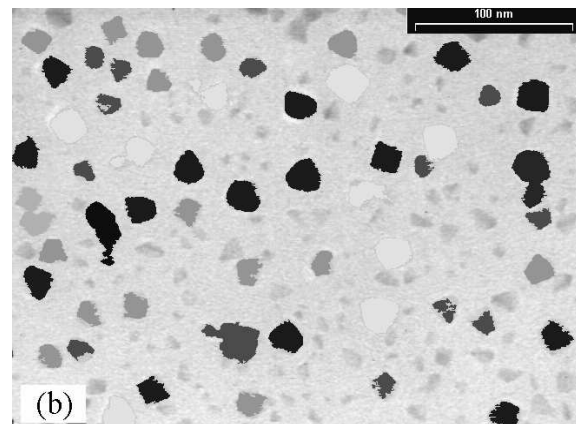
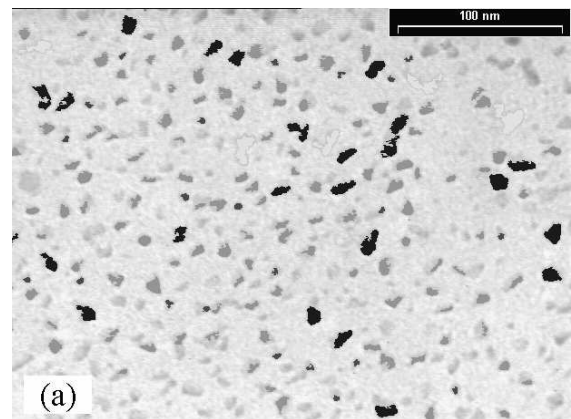


Fig. 2. BF-TEM images of  $\text{Sb}_2\text{O}_3$  thin films: (a)  $d = 0.20 \mu\text{m}$  (b)  $d = 1.10 \mu\text{m}$ .

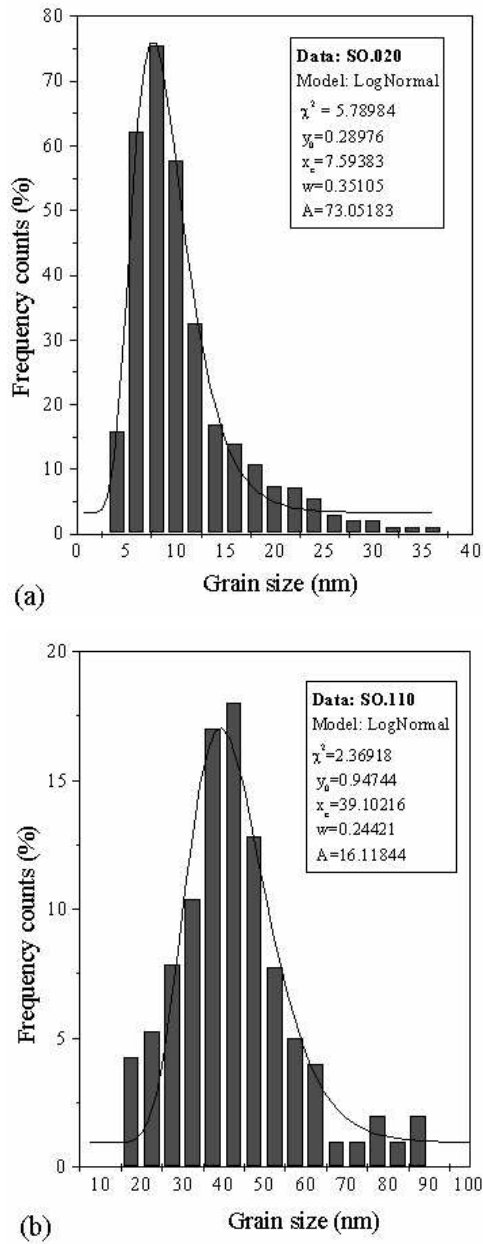


Fig. 3. Grain size distribution of the  $\text{Sb}_2\text{O}_3$  thin films: (a)  $d=0.20 \mu\text{m}$ , (b)  $d=1.10 \mu\text{m}$ .

Surface roughness plays an important role in the optical properties of  $\text{Sb}_2\text{O}_3$  thin films for interferometric applications [17, 18]. The surface morphology of  $\text{Sb}_2\text{O}_3$  thin films was investigated by AFM. Fig. 4a and b show typical surface morphologies of thinner and thicker films, respectively.

The evaluate root mean square (rms) surface roughness of the films, as measured by AFM over a  $3 \times 3 \mu\text{m}^2$  area, were 4.7 nm and 17.6 nm for films with thickness of  $0.20 \mu\text{m}$  and  $1.10 \mu\text{m}$ , respectively. These results indicate that the surface quality of the  $\text{Sb}_2\text{O}_3$  thin

films improvement with decreases of the film thickness. In all cases conical features clearly seen on the films surfaces were the cause of the surface roughness. It is important to note that surface smoothness is a highly desired parameter for the coatings that are used for optical applications in order to reduce the reflection loss due to roughness induced surface scattering [19].

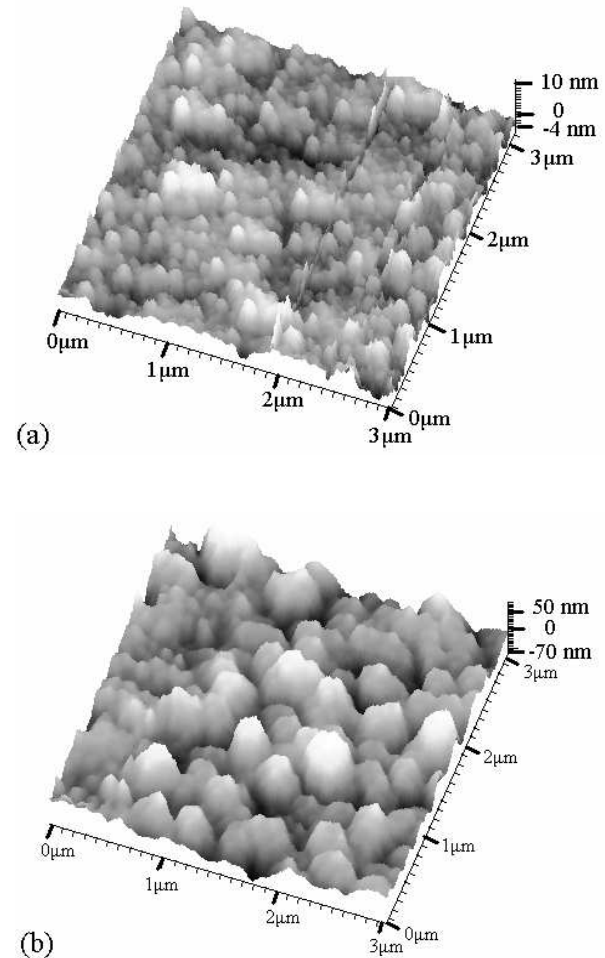


Fig. 4. AFM images of the  $\text{Sb}_2\text{O}_3$  thin films: (a)  $d=0.20 \mu\text{m}$ , (b)  $d=1.10 \mu\text{m}$ .

### 3.2. Optical properties

The optical transmission spectra of the studied  $\text{Sb}_2\text{O}_3$  thin films with different thickness, recorded in wavelength range of 250-1400 nm, are shown in Fig. 5. The transmission spectrum corresponding of thinner film ( $d = 0.20 \mu\text{m}$ ) demonstrates that the film was highly transparent (transmittance  $>85\%$ ) in the visible and near infrared regions. The higher transmittance indicates a fairly smooth surface and relatively good homogeneity of the thinner film, which are consistent with the results of AFM measurements [20].

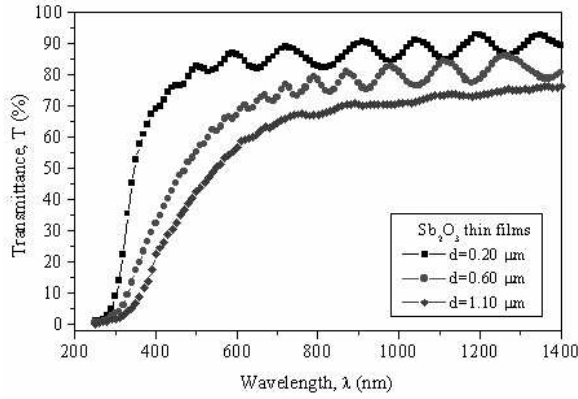


Fig. 5. Transmission spectra of  $Sb_2O_3$  thin films with different thickness.

The appearance of the maxima and minima is due the interference effect from the substrate-film and film-air interferences. The transmittance of the thicker films ( $d=1.10 \mu m$ ) decreases up 75 %. This is because of the reason that in case of thicker films more atoms are present in the film so more states will be available for the photons to be absorbed [21]. When the film thickness is increased the scattering of the light is increased, the coherence between the primary light beam and the beam reflected between the film boundaries is lost and results in the disappearance of the interference which in turn decrease the transmittance of the film [22,23].

It is also observed in Fig. 5 that the transmission curves move toward lower values of wavelength by decreasing the film thickness, indicating that the reduction of the film thickness leads to an increase of the optical band gap,  $E_g$ . Although the thickness does not affect the phase and crystalline structure of the  $Sb_2O_3$  thin films, it seems that the change of optical band gap is basically caused by effect of the thickness on the band structure [24].

The optical absorption coefficient,  $\alpha$ , was calculated from the transmittance data using Swanepoel method [25]. The absorption coefficient of the  $Sb_2O_3$  thin films is was found to be the order  $10^5 \text{ cm}^{-1}$  in the wavelength of 250-350 nm.

For optical applications of semiconducting materials, one of the most important aspect is to determine the range of the wavelength covering the energies of the gaps between the valence and conduction band extreme because it gives the useful information about the region transparency for the film material [3].

According to the Tauc relation [26], the optical band gap energy,  $E_g$ , was determined by plotting  $(\alpha h\nu)^n$  vs. photon energy ( $h\nu$ ) in the high absorption ( $\alpha > 10^4 \text{ cm}^{-1}$ ) range followed by extrapolating the linear region of the plot of  $(\alpha h\nu)^n = 0$ . The exponent  $n$  is an index that characterizes the optical absorption process and is theoretically equal to 1/2, 2, 1/3 or 2/3 for indirect allowed, direct allowed, indirect forbidden and direct forbidden transitions, respectively [27,28]. The best fit to the experimental data was obtained for  $n=2$ . Fig. 6 shows

the plots of  $(\alpha h\nu)^2$  vs.  $(h\nu)$  of the  $Sb_2O_3$  thin films with different thickness.

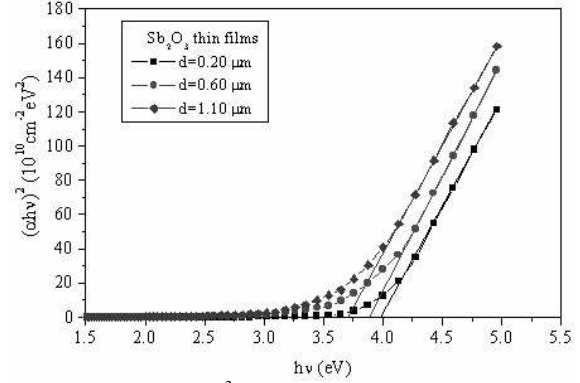


Fig. 6. Plots  $(\alpha h\nu)^2$  vs.  $(h\nu)$  for  $Sb_2O_3$  thin films with different thickness.

The values of optical band gap,  $E_g$ , obtained by extrapolating of the linear region of the plots on the  $h\nu$ -axis are given in Table 1. It was found that the optical band gap of investigated samples decreased from 3.98 eV to 3.71 eV as the film thickness increase from 0.20  $\mu m$  to 1.10  $\mu m$ . The obtained allowed direct transition energy gap values,  $E_g$ , for  $Sb_2O_3$  thin films are in good agreement with the reported values by other workers [3,29,30].

Table 1. Optical and electrical parameters of  $Sb_2O_3$  thin films with different thickness.

Samples $Sb_2O_3$	d ( $\mu m$ )	$D_m$ (nm)	$E_g$ (eV)	$E_a$ (eV)	$\sigma_c$ ( $\Omega^{-1} \text{cm}^{-1}$ )	$\sigma_T$ ( $\Omega^{-1} \text{cm}^{-1}$ )
SO.020	0.20	7.59	3.98	1.02	$1.21 \times 10^{-9}$	$1.52 \times 10^{-3}$
SO.060	0.60	24.38	3.87	0.97	$4.76 \times 10^{-9}$	$1.85 \times 10^{-3}$
SO.110	1.10	39.10	3.71	0.86	$2.24 \times 10^{-8}$	$2.83 \times 10^{-3}$

### 3.3. Electrical properties

The temperature dependence of the electrical conductivity,  $\log \sigma = f(10^3/T)$ , for thin films of  $Sb_2O_3$  with different thickness is shown in Fig. 7. It is clear from these figures, that in all investigated samples; the plots of  $\log \sigma$  vs.  $(10^3/T)$  are straight lines, indicating the conduction in these films through an activated process having single activation energy,  $E_a$ .

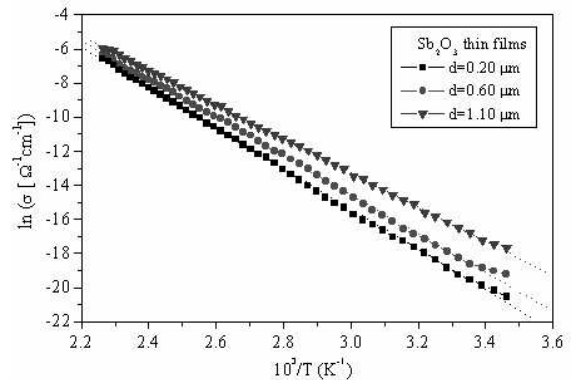


Fig. 7. Temperature dependence of the electrical conductivity of  $Sb_2O_3$  thin films.

The slope of the graph relation  $\sigma = \sigma_0 \exp(-E_a/kT)$  [31], where  $k$  is the Boltzmann constant and  $\sigma_0$  is the pre-exponential factor, determines the values of activation energy  $E_a$ . The calculated values of  $E_a$  are given in Table 1, which also contains the values of electrical conductivity of room temperature,  $\sigma_C$ , and electrical conductivity at 445 K,  $\sigma_T$ . The activation energy of Sb<sub>2</sub>O<sub>3</sub> thin films decreases from 1.02 eV to 0.86 eV as the film thickness increase from 0.20  $\mu\text{m}$  to 1.10  $\mu\text{m}$ .

The decrease in activation energy with increasing film thickness may be due to the change in structural parameters, improvement in crystallite and grain size, decrease in the grain boundaries and removal of some impurities [32]. From Fig. 7 it can be observed that the electrical conductivity decreases with decreasing temperature. Also, from Fig. 7 and Table 1 it can be seen that the value of electrical conductivity tends to increase with increasing film thickness. In particular, there appears a strong increase in the  $\sigma_C$  value from  $1.21 \times 10^{-9} \Omega^{-1}\text{cm}^{-1}$  to  $2.24 \times 10^{-8} \Omega^{-1}\text{cm}^{-1}$  as the film thickness increase to 0.20 to 1.10  $\mu\text{m}$ . At temperature of 445 K the values of electrical conductivity,  $\sigma_T$ , become  $1.52 \times 10^{-3} \Omega^{-1}\text{cm}^{-1}$  for thinner film ( $d = 0.20 \mu\text{m}$ ) and  $2.83 \times 10^{-3} \Omega^{-1}\text{cm}^{-1}$  for thicker film ( $d = 1.10 \mu\text{m}$ ), respectively. The low electrical conductivity of thinner film is attributed to the existence of an island structure, which contain many defect sites. These islands increase in area with the increase of the film thickness leading to the formation of continuous film. This suggests that the defect density is much smaller for thicker films. As results the electrical conductivity of the films increases with increasing film thickness.

#### 4. Conclusions

Sb<sub>2</sub>O<sub>3</sub> thin films have been thermally deposited onto glass substrates kept at room temperature. The thickness of the films was varied from 0.20  $\mu\text{m}$  to 1.10  $\mu\text{m}$ , by changing deposition times. TEM analysis has shown that all investigated samples are polycrystalline in nature having a cubic structure. From BF-TEM and AFM images it was found that the mean grain size and root mean square roughness of films surface increased as the film thickness increased. The variations of optical and electrical parameters such as the optical transmittance, optical band gap energy, electrical conductivity and activation energy of electrical conductivity with film thickness are correlated to the changes in the films microstructure.

#### References

- [1] Y. Zhang, G. Li, J. Zhang, L. Zhang, *Nanotechnology* **15**, 762 (2004).
- [2] K. Ozawa, Y.A. Sakka, J. Amano, *J. Mater. Res.* **13**, 830 (1998).
- [3] N. K. Sahoo, K. V. S. R. Apparo, *Appl. Phys. A* **63**, 195 (1996).
- [4] J. C. G. de Sande, F. Vega, C. N. Afonso, C. Ortega, J. Siejka, *Thin Solid Films* **249**, 195 (1994).
- [5] M. Nalin, Y. Messaddeq, S. J. L. Ribeiro, M. Poulain, V. Briois, *J. Optoelectron. Adv. Mater.* **3**(2), 553 (2001).
- [6] J. Opitz-Coutreau, A. Fielicke, B. Kaiser, K. Rademann, *Phys. Chem. Chem. Phys.* **3**, 3034 (2001).
- [7] N. Tigau, V. Ciupina, G. Prodan, G. I. Rusu, C. Gheorghies, E. Vasile, *J. Optoelectron. Adv. Mater.* **5**(4), 907 (2003).
- [8] N. Tigau, V. Ciupina, G. Prodan, G. I. Rusu, E. Vasile, *J. Cryst. Growth* **269**, 392 (2004).
- [9] N. Tigau, V. Ciupina, G. Prodan, G. I. Rusu, C. Gheorghies, E. Vasile, *J. Optoelectron. Adv. Mater.* **6**(2), 211 (2004).
- [10] N. Tigau, V. Ciupina, G. Prodan, *J. Cryst. Growth* **351**, 987 (2005).
- [11] K. L. Chopra, *Thin Film Phenomena*, McGraw-Hill, New York, (1969).
- [12] G. G. Rusu, *J. Optoelectron. Adv. Mater.* **3**(4), 861 (2001).
- [13] V. Viswanathan, G. G. Rusu, S. Gopal, D. Mangalaraj, *J. Optoelectron. Adv. Mater.* **7**(2), 705 (2005).
- [14] N. Tigau, V. Ciupina, G. Prodan, G. I. Rusu, C. Gheorghies, E. Vasile, *J. Optoelectron. Adv. Mater.* **5**(2), 449 (2004).
- [15] V. Ciupina, I. Carazeanu, G. Prodan, *J. Optoelectron. Adv. Mater.* **6**(4), 1317 (2004).
- [16] N. Tigau, G. I. Rusu, V. Ciupina, G. Prodan, E. Vasile, *J. Optoelectron. Adv. Mater.* **7**(2), 727 (2003).
- [17] D. M. Hausmann, R. G. Gordon, *J. Cryst. Growth* **249**, 251 (2003).
- [18] G. Kiriakidis, N. Katsarakis, M. Bender, E. Gagaoudakis, V. Cimalla, *Mater. Phys. Mach.* **1**, 83 (2000).
- [19] S. Xu, S. Kumar, Y. A. Li, N. Jiang, S. Lee, *J. Phys.: Condens. Matter* **12**, L121 (2000).
- [20] Y. Gao, Y. Masuda, K. Koumoto, *J. Korean Ceramic Society* **40**(3), 213 (2003).
- [21] M. Y. Nadeem, W. Ahmed, *Turk. J. Phys.* **24**, 651 (2000).
- [22] T. K. Subramanyam, B. Srinivasulu Naidu, S. Uthanna, *Cryst. Res. Technol.* **34**(8), 981 (1999).
- [23] S. H. Jeong, J.W. Lee, S. B. Lee, J. H. Boo, *Thin Solid Films* **435**, 78 (2003).
- [24] J. Sandino, G. Gordillo, *Surf. Rev. Letter.* **9**(5/6), 16 (2002).
- [25] R. Swanepoel, *J. Phys. E: Sci. Instrum.* **16**, 1214 (1983).

- [26] T. S. Tauc, A. Memth, J. Non-Cryst. Solids **126**, 569 (1972).
- [27] K. Bindu, J. Campos, M. T. S. Nair, A. Sanchez, P. K. Nair, Semicond. Sci. Technol. **20**, 496 (2005).
- [28] A. F. Quasrawi, Cryst. Res. Technol. **40**(6), 610 (2005).
- [29] C. Wood, B. Van Pelt, A. Dwight, Phys. Stat. Sol. (b) **54**, 701 (1972).
- [30] B. Wolffing, Z. Hurych, Phys. Stat. Sol. (a) **16**, K161 (1973).
- [31] N. F. Mott, E. A. Davis, Electronic Processes in Non-Crystalline Materials, Calderon Press Oxford, (1979).
- [32] R. B. Kale, C. D. Lokhande, Semicond. Sci. Technol. **20**, 1 (2005).

---

\* Corresponding author: [ntigau@ugal.ro](mailto:ntigau@ugal.ro)